

OBSERVATIONS OF QUASI-COHERENT SOFT X-RAY OSCILLATIONS IN U GEMINORUM
AND SS CYGNIF. A. CORDOVA,¹ T. J. CHESTER,² K. O. MASON,³ S. M. KAHN,⁴ AND G. P. GARMIRE⁵

Received 1982 September 13; accepted 1983 August 26

ABSTRACT

Soft X-ray pulsations (0.1–0.5 keV) have been detected for the first time from U Geminorum and for the second time from SS Cygni using the *HEAO 1* satellite. Both dwarf novae were on the declining phase of an optical outburst. The average amplitudes of the pulses are 15% for U Gem and 18% for SS Cyg. The pulsations are quasi-coherent in character. If we define P_c to be the centroid of the period distribution and P_1 to be the standard deviation of the pulsation period (and, hence, a measurement of the width of the period distribution), then during the U Gem observation $P_c = 27$ s and $P_1 = 6$ s, while during the SS Cyg observation $P_c = 10.7$ s and $P_1 = 1.8$ s. In a previous X-ray observation of SS Cyg, an oscillation with $P_c = 8.8$ s and $P_1 = 0.4$ s was detected, illustrating that significant changes in period and coherence may occur.

A blackbody spectral fit to the U Gem data yields best fit parameters of $kT \sim 25$ eV, $N_H \leq 5 \times 10^{18}$ cm⁻², and a 0.13–0.48 keV X-ray flux at the Earth of 3×10^{-10} ergs cm⁻² s⁻¹. From pulse phase X-ray spectroscopic data, an upper limit of 50% may be set on any variation in temperature across U Gem's pulse. There is no evidence for an X-ray variation correlated with the optical eclipse of this 4.25 hr binary system.

The average soft X-ray flux of SS Cyg during the second *HEAO 1* pointing observation is $f_x \sim 2 \times 10^{-11}$ ergs cm⁻² s⁻¹, one-half that detected in the first *HEAO 1* soft X-ray pointing at this star.

We review all the data on the X-ray and optical pulsations thus far detected in these two dwarf novae and discuss the observational constraints on various current models for the pulsations.

Subject headings: stars: accretion — stars: dwarf novae — stars: pulsation — stars: U Geminorum — stars: variables — X-rays: binaries

I. INTRODUCTION

Cataclysmic variable stars are believed to be close binary systems containing a degenerate dwarf star accreting material from an accretion disk that is fed by a Roche lobe filling late-type companion. The dwarf novae are a subset of cataclysmic variables that undergo frequent optical brightenings, or "outbursts," of amplitude 2–5 visual magnitudes. The typical outburst recurrence times are a few weeks or months (see reviews by Robinson 1976; Warner 1976; Córdoba and Mason 1983). The rise to peak visual light usually occurs in less than a day, and the emission thereafter declines more slowly to the preoutburst light level over the course of a few days.

Soft X-ray (0.1–0.5 keV) emission has been observed from the dwarf novae SS Cygni (Rappaport *et al.* 1974; Hearn, Richardson, and Li 1976; Margon *et al.* 1978) and U Geminorum (Mason *et al.* 1978) during optical outbursts. Hard X-ray (>2 keV) emission has also been detected from these stars (e.g., Ricketts, King, and Raine 1979; Swank 1979). Córdoba *et al.* (1980a, hereafter Paper I) obtained an X-ray pointing observation of SS Cyg with the *HEAO 1* satellite during an outburst in 1978 June. They found that SS Cyg's soft X-ray emission was pulsed with a period close to 9 s, but that the pulsation was unstable; they noted that

the deviations from coherence could be described mathematically as a random walk in the phase of the pulse. The short period and high temperature of the oscillations suggest that the pulsed emission originates in the vicinity of the degenerate dwarf star.

Short-period optical oscillations with amplitudes $\leq 2\%$ are observed in many dwarf novae, including SS Cyg and U Gem, during outbursts (Robinson and Nather 1979, hereafter RN; Patterson 1981). The exact relationship of the X-ray to the optical oscillations has not yet been determined.

In § II we report on a *HEAO 1* X-ray pointing observation of U Geminorum, and a second *HEAO 1* pointing observation of SS Cygni. Both observations were made when the target star was in optical outburst, and in both cases quasi-coherent oscillations were detected in the soft X-ray flux. In § III we discuss the mathematical methods we used to derive the pulse parameters. In § IV the X-ray observations are compared with the optical observations and various mathematical models which have been proposed to describe the behavior of the optical pulsations are evaluated in light of the X-ray data.

II. OBSERVATIONS

The X-ray data reported here were taken with the low-energy detector, LED 1, of the *HEAO 1* A-2 experiment which is described in detail by Rothschild *et al.* (1979). LED 1 was a collimated gas proportional counter with sensitivity in the energy range 0.1–3.0 keV. A special collimator design whereby sources were viewed simultaneously with $1.5 \times 3^\circ$ and $3^\circ \times 3^\circ$ fields of view made it possible to infer the separate contributions from a source and the X-ray sky

¹ University of California, Los Alamos National Laboratory.² Jet Propulsion Laboratory.³ University College London, Mullard Space Science Laboratory.⁴ Columbia Astrophysics Laboratory and Department of Physics, Columbia University.⁵ Pennsylvania State University.

background even when the detector was pointed at a single position in the sky. Aspect information acquired from an on-board star tracker was used to determine the position of the source in the detector collimator and to correct the X-ray signal for the effect of small changes in the pointing direction of the spacecraft during the course of the observation.

a) *U Geminorum*

HEAO 1 was pointed at U Gem for 10 hr commencing at 09:30 UT on 1978 October 16, about 2 days after the peak of an optical outburst which lasted several days. The visual light curve of U Gem's outburst, based on data supplied by the AAVSO, is shown in Figure 1 (center). The X-ray observation consisted of seven satellite orbits of ~ 90 minutes each, referred to here as ORB 1-7, respectively. Useful data were obtained from ~ 30 -40 minutes per orbit. Most of the data were obtained with the detector gain set so that the lowest pulse height threshold occurred at an energy of 0.18 keV ("normal" gain). However, for part of ORB 5, 6, and 7, the detector gain was increased so that the low-energy threshold was reduced to 0.13 keV ("high" gain). Broad-band data were accumulated in 1.28 s integrations. In addition, during ORB 2-6, a special telemetry mode was used that allowed direct pulse-height readouts of individual photon events up to a maximum of one per 20 ms. These data are not useful for analysis of intensity variability because the signal is saturated, but they can be used to provide information on the shape of the spectrum as a function of time. During ORB 1 and 7, properly normalized spectral data are available with 10.24 s time resolution.

i) Light Curve

The background-subtracted, aspect-corrected light curve of U Gem during the *HEAO 1* observation is plotted in Figure 2. The points represent summations over 40.96 s of data accumulated in the broad-band energy ranges 0.18-0.43 keV (Fig. 2a) and 0.13-0.28 keV (Fig. 2b). These energy ranges correspond to different high voltage settings on the detector anode as noted above.

Figure 2a indicates that the 0.18-0.43 keV flux from U Gem decreased by about a factor of 2 over the first 6 hr of the X-ray observation. The high-gain data (Fig. 2b) exhibit a $\sim 24\%$ monotonic flux increase over the last 4 hr of the

observation, while the quasi-simultaneous low-gain data (Fig. 2a) show no more than a 5% increase over the same time period. We have investigated whether the relative change in flux in the different energy bands could be accounted for by a change in the spectrum of the source by folding trial spectra through the response curve of the detector and comparing the predicted flux in the two energy bands of interest as a function of the spectral parameters. Independent estimates of the allowed range of temperature from the normal and high-gain data are consistent to within about 50%, and variations within this range are not sufficient to produce the change in the ratio of high- and normal gain data observed. A variation in N_H from $\sim 10^{20}$ to $\leq 10^{19}$ will produce the desired change in the ratio. However, this would be accompanied by an increase in the measured flux by a factor of about 4, which is not observed. Thus, in order to explain the data in terms of an astrophysical cause, we require a decrease in column density with a concomitant decrease in the spectral normalization: a rather contrived situation. Alternatively, there may be another, extremely soft, point source within the field of view which is only recorded in high-gain mode. The only other explanation is that the effect is instrumental (e.g., electron contamination; cf. Appendix A of Córdoba 1979). This cannot be eliminated, since there are very few data on the behavior of the LED detector at high gain.

There is no evidence for variability commensurate with the binary period of the system (4.25 hr), nor is there evidence for the factor of 10 or greater variability found by Mason *et al.* (1978) in *HEAO 1* scanning observations of U Gem taken during the early part of an outburst in 1977.

ii) Short Time Scale Variability

A representative portion of the light curve of U Gem is plotted with a much shorter time resolution of 1.28 s in Figure 3b. It is evident that the X-rays are highly modulated on time scales of 20-30 s. For comparison, a partial light curve of SS Cyg during the 1978 June outburst, when 9 s oscillations were observed, is shown in Figure 3a.

The time series for each satellite orbit of U Gem data were Fourier transformed. A representative power spectrum is shown for ORB 5 in Figure 4a; it exhibits a broad peak of power suggesting a quasi-periodic oscillation. Summed power

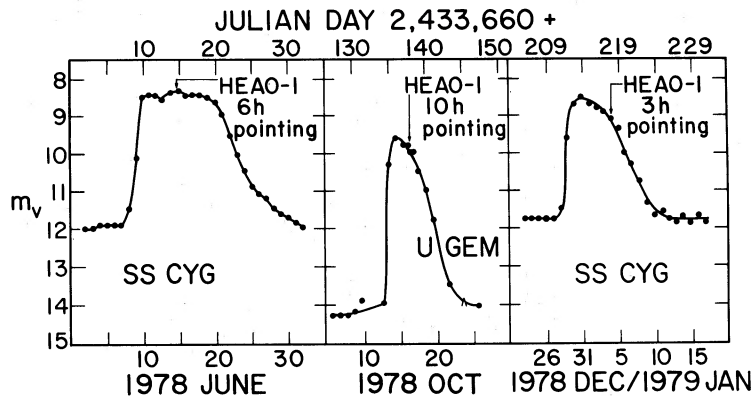


FIG. 1.—Optical light curves from data supplied by the AAVSO show when, during the outbursts of SS Cyg (left and right) and U Gem (center), the *HEAO 1* X-ray observations were made.

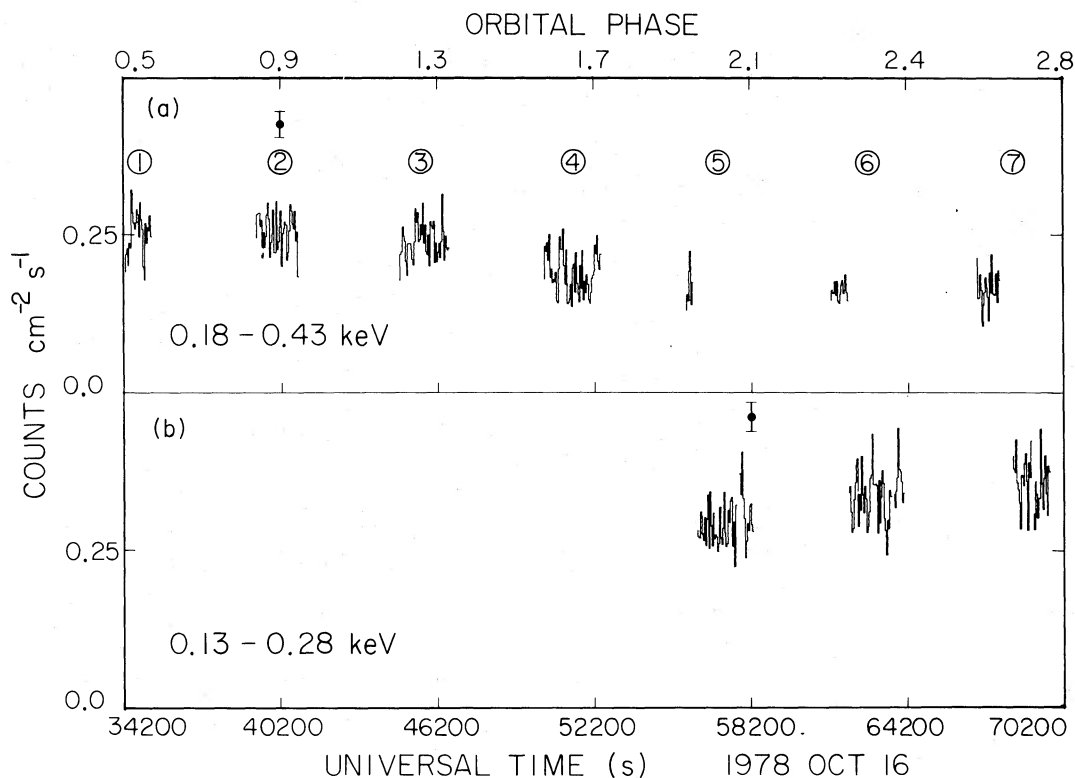


FIG. 2.—The soft X-ray light curve covering the entire *HEAO 1* 10 hr pointing at U Geminorum. The data have been corrected for aspect, and the X-ray sky background has been subtracted. Each data point is an average over 40.96 s of data. The dropouts are due to Earth occultations. Each satellite orbit (~ 90 minutes in duration) is labeled 1, 2, etc. The data in the top and bottom panels were taken when the high voltage on the detector anode was at different settings (see text), resulting in different effective energy bandpasses. A representative error bar is shown above the second segment of continuous data in the top panel and above the first data segment in the bottom panel. The orbital phase was calculated using the ephemeris of Arnold, Berg, and Duthie (1976).

spectra for ORB 1–5 and ORB 6–7 are displayed in Figures 4b and 4c, respectively. These particular orbits were combined in order to illustrate that the centroid of the power excess changes on relatively short time scales: the peak in ORB 1–5 is centered on ~ 25 s, whereas in ORB 6–7 it is centered on ~ 29 s (this is also shown in Figure 8 which is discussed later).

iii) The Spectrum

For the spectral analysis we used data taken with the higher gain setting. In Figure 5 the observed count rate spectrum from ORB 7 and the best fit blackbody model, which had a temperature $kT = 25$ eV and a column density $N_H \leq 5 \times 10^{18} \text{ cm}^{-2}$, are shown. The inset to Figure 5 displays the 90% confidence contours for fits to both a blackbody spectrum and a thermal bremsstrahlung spectrum (i.e., exponential plus Gaunt factor), assuming Brown and Gould (1970) cross sections for interstellar absorption. The limits on the source temperature are:

$$5.04 < \log T < 5.47 \text{ (blackbody)}$$

$$5.15 < \log T < 5.78 \text{ (thermal bremsstrahlung).}$$

The detector is insensitive to a decrease in N_H below $\sim 5 \times 10^{18} \text{ cm}^{-2}$; thus both models are consistent with zero hydrogen column density. The 90% confidence upper limit to

N_H for both models is $2.5 \times 10^{20} \text{ cm}^{-2}$. These results are consistent with those of Mason *et al.* (1978) derived from previous *HEAO 1* scanning data taken in the normal gain setting.

The flux at the Earth in the energy interval 0.13–0.48 keV is $3.4 \times 10^{-10} \text{ ergs cm}^{-2} \text{ s}^{-1}$, assuming the best fit spectral parameters from either model. The total luminosity inferred in the blackbody component is extremely sensitive to the exact spectral parameters chosen (see, e.g., Tuohy *et al.* 1978), since at temperatures of a few eV most of the flux is emitted outside the energy range of the *HEAO 1* detectors. Using the best fit blackbody parameters ($kT = 25$ eV, $N_H \leq 5 \times 10^{18} \text{ cm}^{-2}$), the luminosity at the source, integrated over all frequencies, is $2 \times 10^{33} \times (d/100 \text{ pc})^2 \text{ ergs s}^{-1}$. However, this increases to $\sim 10^{35} \times (d/100 \text{ pc})^2 \text{ ergs s}^{-1}$ at the lowest extreme of temperature allowed by the spectral fitting (inset to Fig. 5). A distance of 100 pc is consistent with the low N_H value from the X-ray observation and the value of ~ 75 pc calculated by Wade (1979) for U Gem based on optical spectrophotometry.

To search for evidence of spectral variability associated with the ~ 25 s pulsations, we used the spectral data taken in the 20 ms resolution mode during ORB 2–6. In this mode, incoming photons are tagged with a number between 0 and 63 that depends on their energy (pulse height), and the information for the last photon event recorded in each 20 ms

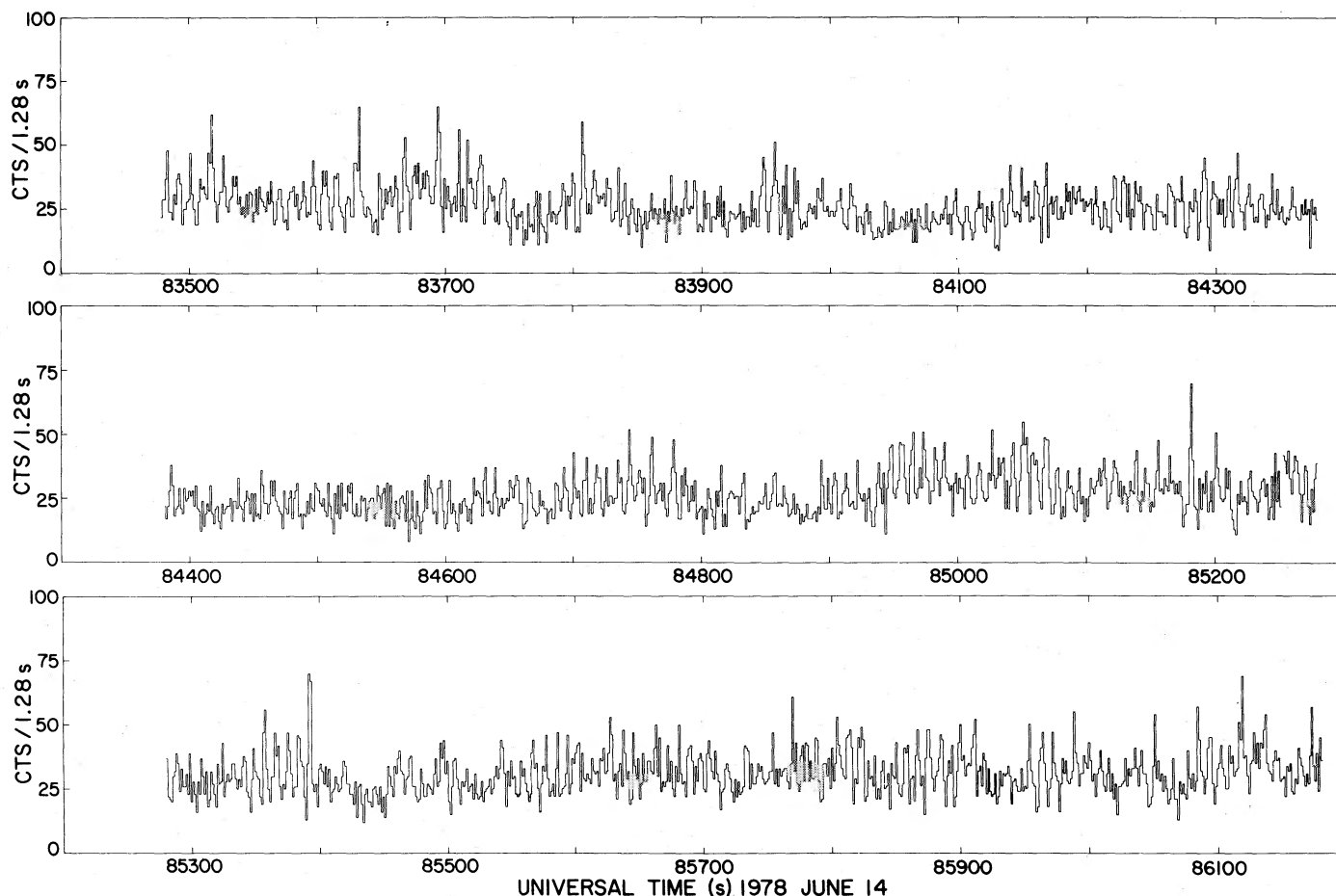


Fig. 3a.—A portion of the soft X-ray light curve for SS Cygni during the 1978 *HEAO 1* pointing observation, in 1.28 s binning.

interval is telemetered to Earth. It is thus possible to obtain integrated phase-resolved spectra for recurrent, short time scale phenomena. We constructed two such 64 channel pulse-height spectra, one derived from data obtained near the maxima of the pulses, as determined from the pulse arrival times calculated using the 1.28 s resolution data, and the other from the interpulse region. The slope of these spectra is parameterized by taking the ratio of counts in the energy range 0.25–0.43 keV to those in the range 0.18–0.25 keV. This ratio is the same in both instances to within 30%. Taking into account the resolution and response of the detector, this corresponds to a 50% limit on a change in temperature. No evidence is found for changes in the spectrum on an orbit to orbit basis during ORB 1–7 to a similar level of accuracy.

b) SS Cygni

A *HEAO 1* pointing observation of SS Cygni was conducted on 1979 January 4 from 0–3 hr UT. The source was declining from an optical outburst which began on 1978 December 28 (± 1 day). Figure 1 (right) shows the AAVSO light curve for the outburst with the time of the X-ray observation noted.

HEAO 1 reentered the Earth's atmosphere about 2 weeks after this observation; the low altitude of the satellite orbit (~ 350 km) during this time rendered much of the X-ray

data unusable because of contamination from the Earth's albedo during the daylight portions of the orbit. Three sections of good quality night time data, each of 10 minutes duration and separated by intervals of ~ 1.3 hours, were available for analysis; these are shown with 1.28 s resolution in Figure 3c. All data were accumulated in the normal gain mode (cf. § IIa). The count rate was $0.025 \text{ cm}^{-2} \text{ s}^{-1}$; this is about one-half the intensity observed in the previous 1978 *HEAO 1* observation, or $\sim 2 \times 10^{-11} \text{ ergs cm}^{-2} \text{ s}^{-1}$. It was not possible to fit model spectra to these data because of the low count rate of the source and the relatively small amount of usable data.

Fourier transforms were made of each of the three sections of data. Each transform contained 512 1.28 s bins (less than 10% of the data stream had to be padded with the average value of the data to complete the 2^9 point transform). The resulting power spectra were superposed to yield the average spectrum shown in Figure 6. A broad peak is apparent, centered on 10.7 s. It is similar to the excess in the power spectrum of U Gem (Fig. 4).

III. ANALYSIS OF THE PULSATIONS

The observations indicate quasi periodicity instead of a strict periodicity. As discussed later in § IV, a number of possible explanations for behavior of this sort have been suggested on both physical and mathematical grounds. In Paper I the

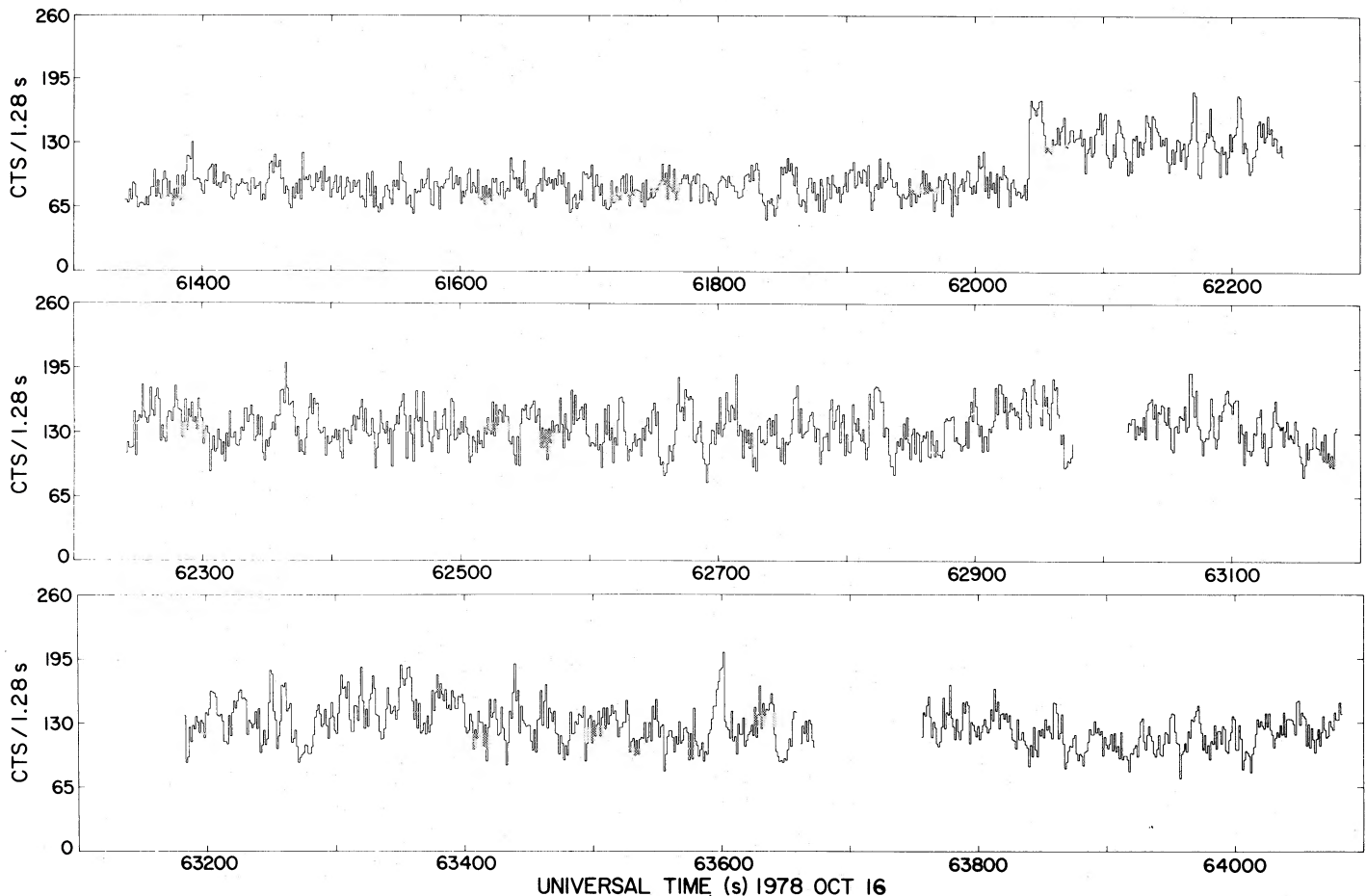


FIG. 3b.—The same as Fig. 3a, but for U Gem during the 1978 October *HEAO 1* pointing; the abrupt rise in count rate at 62,400 s is due to a change from a lower to a higher detector gain.

quasi coherence of SS Cyg was modeled by a random walk process in the phase of the pulsation. Such a model can reproduce the shape of the power spectra exhibited in Figures 4 and 6 and can yield simulated time series which qualitatively resemble the U Gem and SS Cyg data sets presented in this paper. Analysis of the observations in terms of a random walk in phase or frequency is straightforward and yields a single parameter characterizing the strength of the random walk. Unfortunately a variety of different detailed stochastic processes may yield the same random walk parameters, complicating the interpretation of the results.

As shown below, no single method of analysis is appropriate for all three of the X-ray pulsation data sets (i.e., the two observations of SS Cyg and the observation of U Gem). We present different methods that obtain the random walk parameters for each data set and discuss the relative merits of the methods.

a) Noise Parameters Derived from a Superposition of Pulse Trains

One method that can be used to distinguish between random walk noise in phase, frequency, or higher derivations is to examine the time dependence of the variance in phase residuals $\langle \delta\phi^2(t) \rangle \equiv \langle \phi^2(t) \rangle - \langle \phi(t) \rangle^2$. In Paper I, an

analog of $\langle \delta\phi^2(t) \rangle$ was measured for the SS Cyg pulsations using the pulse arrival times. A linear dependence on time was derived, which favors a random walk in phase. Unfortunately, it is not possible to perform a similar analysis for the U Gem data set or the more recent SS Cyg data set because the pulsations are substantially less stable. One cannot uniquely specify the relative phase of two pulsations over durations longer than ~ 10 cycles in the case of U Gem, while the signal-to-noise ratio in the second SS Cyg observation (1979) is too low for arrival times for individual pulses to be deduced.

For the U Gem data, in which individual pulses can be distinguished, we have developed a method for determining the noise parameters for a general random walk model which makes use of all of the data, not just the arrival times. It is, consequently, a more general method than that described in Paper I.

A pulse train whose phase varies in a random manner can be represented by

$$f(t) = g(\omega t + \phi_t), \quad (1)$$

where ϕ_t is the phase shift at time t resulting from the random walk in phase, frequency, or higher derivatives, and g is an arbitrary function of phase representing the pulse shape. If N such pulse trains are superposed so that their

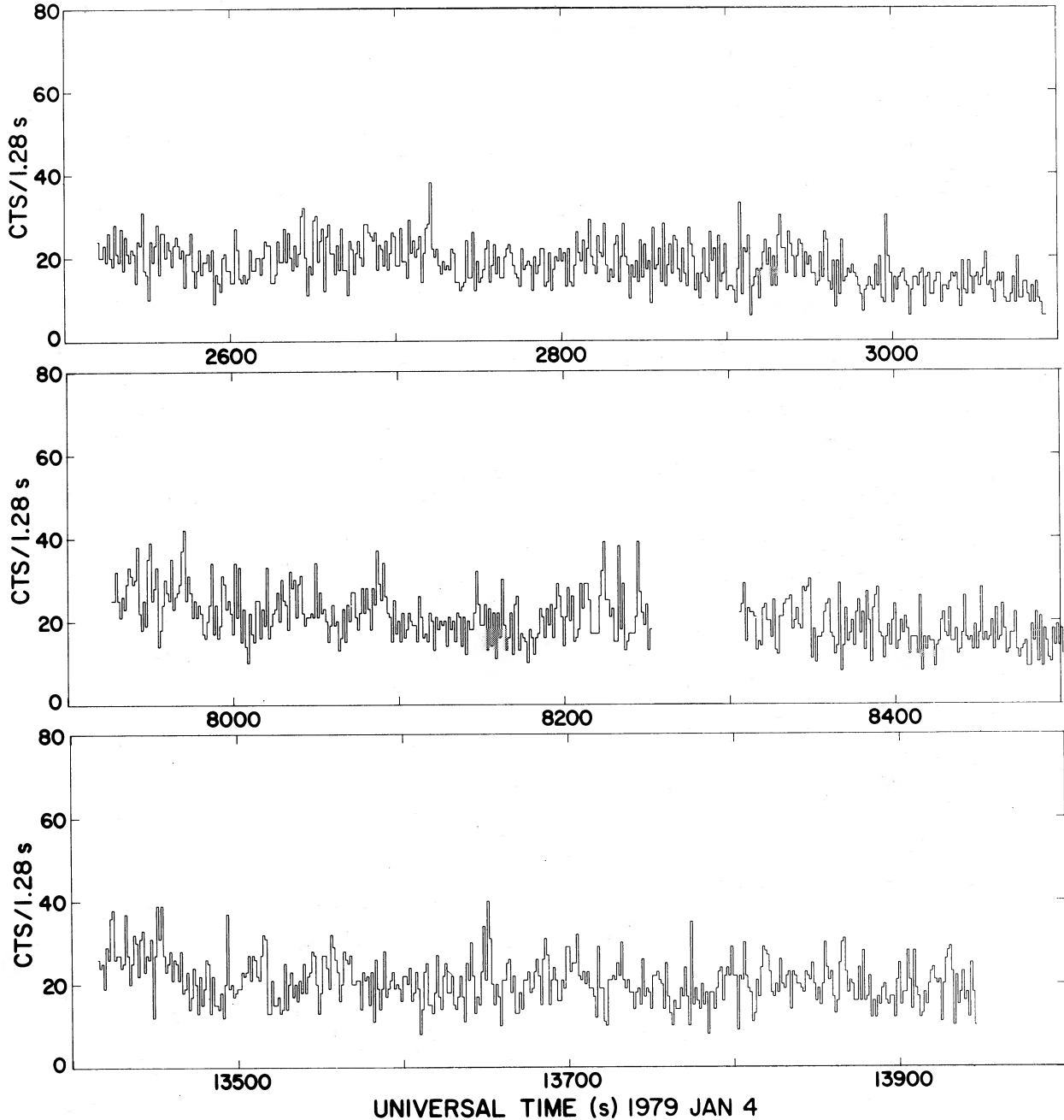


FIG. 3c.—The same as Fig. 3a, but for SS Cyg during the 1979 January *HEAO 1* pointing

peaks at $t = 0$ coincide and the result is divided by N , the expectation of the resulting function is

$$F(t) = \langle g(\omega t + \phi_t) \rangle. \quad (2)$$

The function $g(\omega t + \phi_t)$ can be expanded in terms of its harmonics:

$$g(\omega t + \phi_t) = \sum_{n=0}^{\infty} a_n \cos(n\omega t + \phi_n + \phi_t).$$

Then,

$$\begin{aligned} \langle g(\omega t + \phi_t) \rangle &= \sum_{n=0}^{\infty} a_n \cos(n\omega t + \phi_n) \langle \cos \phi_t \rangle \\ &= g(\omega t) \langle \cos \phi_t \rangle, \end{aligned}$$

since $\langle \sin \phi_t \rangle = 0$ if ϕ_t is a random walk variable.

If the random walk steps occur very frequently, then the Central Limit Theorem guarantees that the probability

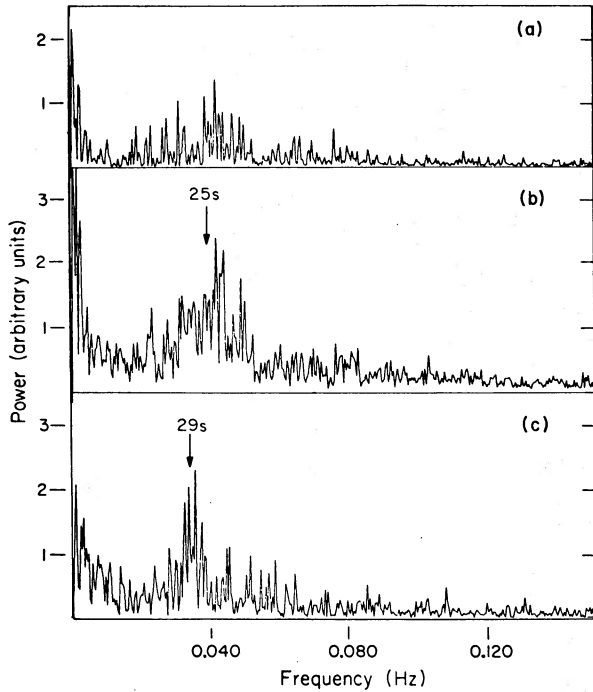


FIG. 4.—Power spectra for U Gem resulting from discrete Fourier transform of (a) a single satellite orbit (ORB 5), (b) ORB 1–5, and (c) ORB 6–7. For (b) and (c), the power spectra of each orbit of data were added together.

distribution in $\phi(t)$ is nearly Gaussian. A straightforward calculation then gives:

$$\langle \cos \phi_i \rangle = e^{-\langle \phi_i^2 \rangle / 2} \quad (3)$$

From Cordes (1980) we have:

$$\langle \phi_i^2 \rangle = S_\phi |t| \quad \text{for phase noise,} \quad (4)$$

$$\langle \phi_i^2 \rangle = \frac{1}{3} S_\omega |t|^3 \quad \text{for frequency noise,} \quad (5)$$

and

$$\langle \phi_i^2 \rangle = \frac{1}{20} S_s |t|^5 \quad \text{for noise in the frequency derivative.} \quad (6)$$

Here S_ϕ , S_ω , and S_s are the intrinsic strengths of the random walks and are equal to the product of the step rate and the mean-squared step amplitude for each case.⁶ Thus the logarithm of the envelope of $F(t)$ will be linear with time for phase noise, a cubic for frequency noise, and a quintic for noise in the second derivative. Similar dependences on “ t ” apply to the function $\langle \delta\phi^2(t) \rangle$ used in the method described in Paper I. In general, one can perform a fit to an expression proportional to $|t|^\alpha$ and confidence limits can be specified on α . Note that all of the data can be included in a fit to $F(t)$, not only the pulse arrival times. Thus this method is more sensitive than

⁶ It should be emphasized that eq. (3) is valid only if the step rate is large compared to t^{-1} . If this is not the case, higher moments must be included in the argument of the exponential, but only for the frequency noise and second-derivative noise cases.

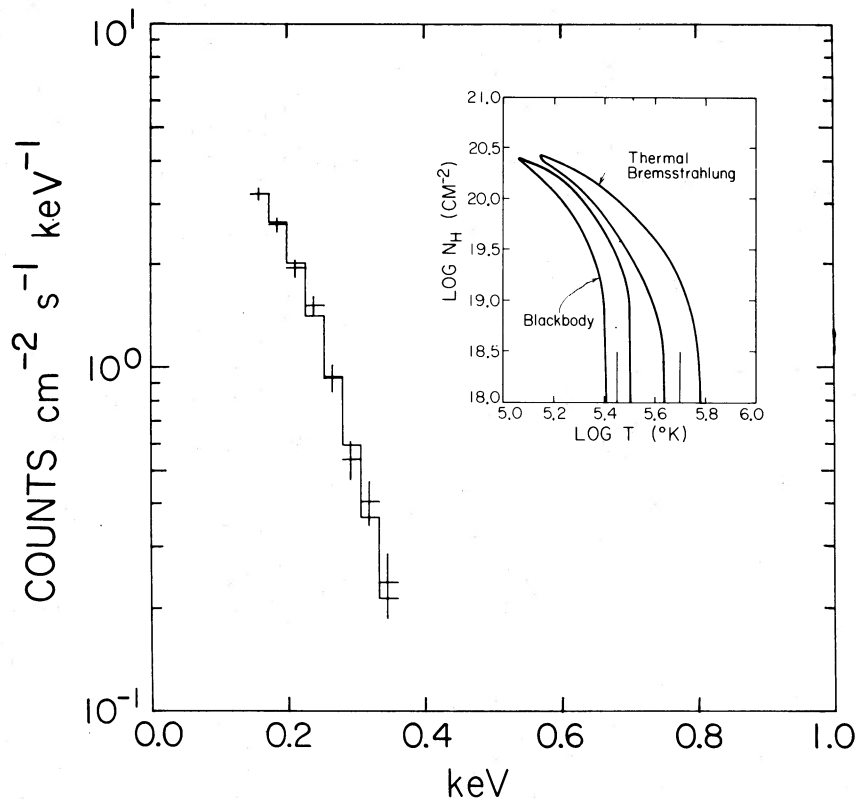


FIG. 5.—The observed energy spectrum for U Gem (crosses) and the best-fit blackbody spectrum (solid line), which has a $kT \sim 25$ eV and $N_H \leq 5 \times 10^{18} \text{ cm}^{-2}$. The inset shows the 90% confidence χ^2 contours for both blackbody and thermal bremsstrahlung (plus Gaunt factor) fits.

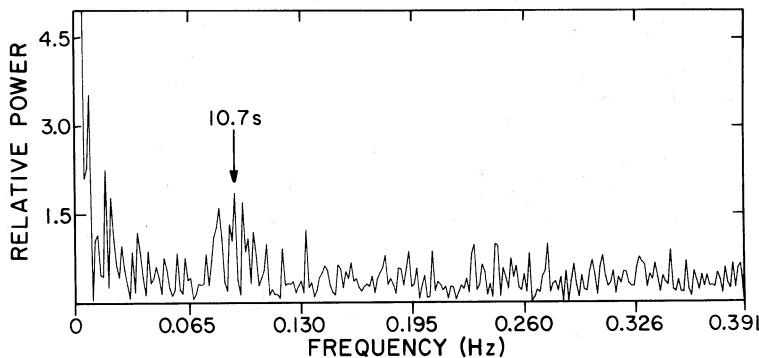


FIG. 6.—The summed power spectrum from the three sections of data displayed in Fig. 3c for the SS Cyg 1979 January observation

that involving explicit measurement of $\langle \delta\phi_i^2 \rangle$. Note as well that the pulse shape structure (“ g ” in eq. [1]) is preserved by this analysis.

An estimate of $F(t)$ can be formed in the following way. We first derive t_i , the time of maximum for each pulse. Then we construct

$$F_{\text{est}}(t) = \frac{1}{N} \sum_{i=1}^N f(t - t_i), \quad (7)$$

where f is an observed continuous data train (for example, one of the ORB sections), and N is now the number of pulses in the data train. Thus for every pulse in a given pulse train, the entire pulse train is superposed on itself, with every pulse acting once in turn as the center of the superposition. Finite pulse trains can easily be taken into account by a normalization using the number of data points in each bin of the superposition.

Of course, $F(t)$ is obtained by adding independent pulse trains, whereas $F_{\text{est}}(t)$ is obtained by adding the same pulse train to itself many times with different phase shifts. These approaches are identical only if ϕ_i is uncorrelated with $\phi_{i+\tau}$ for any τ . For a pulse train with a random walk in phase, the assumption will hold for long time intervals but not for short ones. The difference between $F(t)$ and $F_{\text{est}}(t)$ can be calculated analytically or derived from simulated data. For the analyses in this paper, $F_{\text{est}}(t)$ is shown to be a good estimate of $F(t)$ by the agreement between the parameters we deduce for SS Cyg (1978) from this approach and the parameters deduced independently in Paper I. Because the other time series observed for U Gem and SS Cyg exhibit less coherent pulsations, this assumption should then hold true for analyses of those data sets as well.

There is, however, some contamination due to the effects of counting statistics. Uncertainties due to counting statistics introduce a white noise contamination which decreases the amplitude of the damped sinusoid because it shifts the observed arrival time t_i away from the true arrival time by some random amount σ_i . For $t \neq 0$, $F_{\text{est}}(t)$ becomes

$$F_{\text{est}}(t) = A \langle \cos \omega \sigma_i \rangle e^{-\langle \phi_i^2 \rangle / 2} g(\omega t). \quad (8)$$

Thus the measured amplitude includes an average attenuation due to errors in the pulse arrival times. The pulse centered on $t = 0$, however, has an *increased* amplitude because the pulse arrival times are chosen to be the times when the count rate is maximal. These noise effects are important only when the

noise due to counting statistics is comparable to the pulsation amplitude.

Plots of the function, $F(t)$, derived from selected orbits of data on SS Cyg (1978) and U Gem are displayed in Figure 7. If we set $g(\omega t) = \cos(\omega t)$, then in both cases the first order expression for $\langle \phi_i^2 \rangle$ (eq. [4]) provides a substantially better fit compared to the higher order models (eqs. [5] and [6]). Thus models involving a random walk in phase as opposed to frequency or higher derivatives are favored by the data. Plots of the residuals to the fits to $F(t)$ (assuming eq. [4] applies) are displayed in Figures 7c and 7d. This fit was statistically acceptable for the 1978 SS Cyg data set as long as the zero-centered pulse is excluded. For the U Gem data the fits are acceptable even if the zero offset pulse is included.

We have fitted all of the orbits of data in a similar manner and display the fitted parameters in Figures 8a (SS Cyg 1978) and 8b (U Gem). Shown together with the random walk strength (S_ϕ) are the average intensities in counts $\text{cm}^{-2} \text{s}^{-1}$ (I), the pulsed fractions (A), and the periods (P) for each ORB. The last three quantities were derived using $F(t)$ from the fits.

The random walk strength found for the SS Cyg 1978 data set using the pulse train superposition method agrees with the strength deduced in Paper I by other means. The amplitudes and periods are also consistent with our previous determinations. The periods found through fits to $F(t)$ are not identical to the intrinsic periods of the oscillation when only a finite number of pulses are superposed because the statistical nature of the phase noise can lead to uncertainties in parameter determination for finite samples.

b) Noise Parameters Derived from the Power Spectrum

When the strength of the oscillating signal is too low to determine pulse arrival times neither the method of examining the variance of the pulse phase with time (as was done in Paper I), nor the method of superposition of pulses described above, is appropriate. One must then resort to a cruder technique of deriving the noise parameters from the power spectrum.

The 1979 observations of SS Cygni is a case in point. It is simple enough to use Figure 6 to determine the mean period from the centroid of the peak and to determine the pulsation amplitude from the integral of the excess power in the broad peak. However, to derive the noise strength of the pulsation from the power spectrum alone we must adopt a model noise process for the oscillation. We assume that, by analogy with

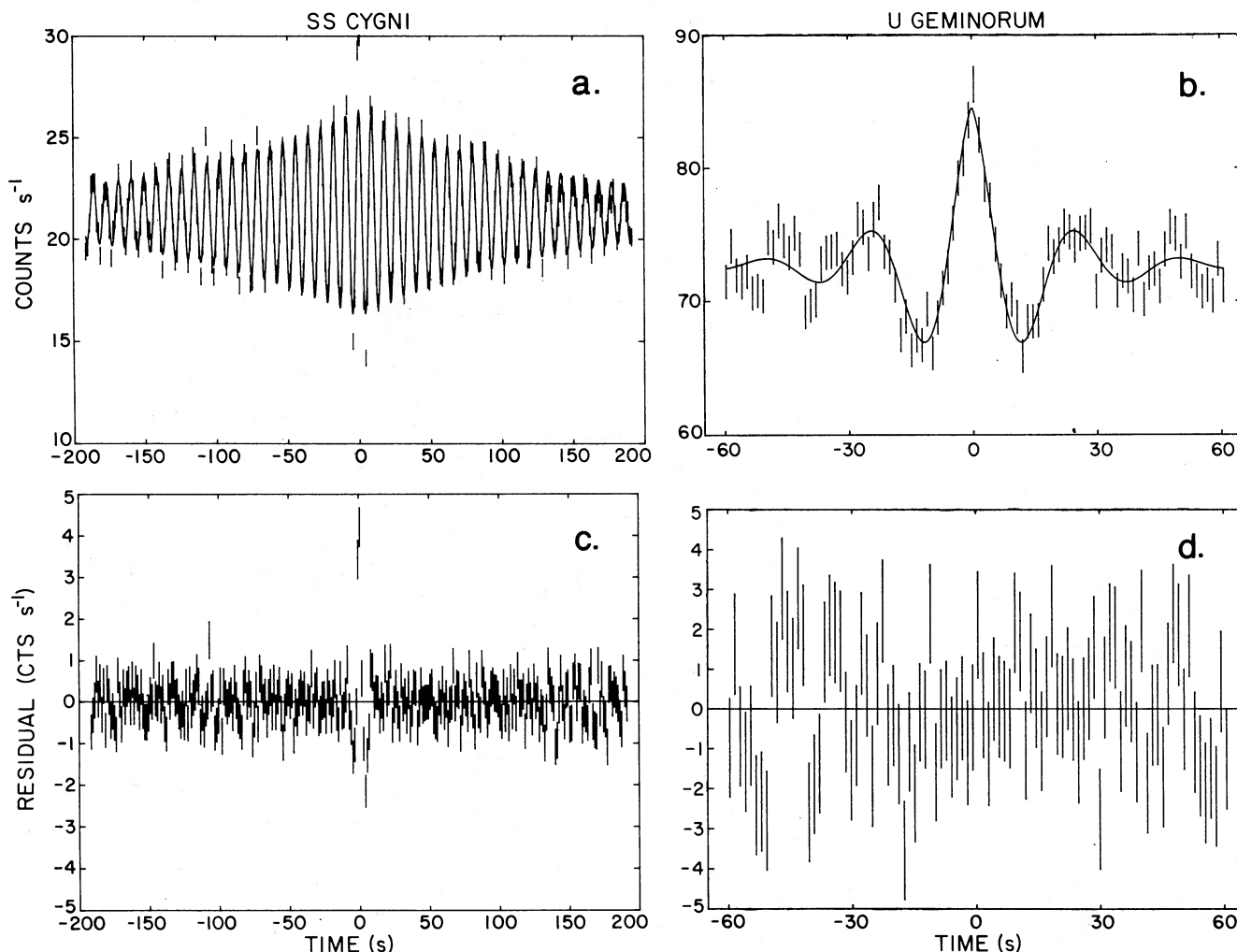


FIG. 7.—The results from fitting a function of the form $F(t) = e^{-S|t|/2} \cos(\omega t)$, where S is the strength of the random walk in phase, to the superposition of dwarf nova pulse trains. Figs. 7a and 7c show the functional fit (solid line) to one orbit (ORB 2) of SS Cyg data (bars) from the earlier, 1978 June observation, and the residuals to the fit. Figs. 7b and 7d are similar plots for one orbit (ORB 4) of U Gem data. The fits show that the strength of the random walk is much stronger in U Gem than in the first SS Cyg pointing observation.

the previous X-ray observations of U Gem and SS Cyg, the broad power distribution is produced by phase noise. We then construct a mathematical model for a random walk in phase and use it to generate artificial data; of course, this is only one of several possible random walk models (see § IV). In the model the pulsation period and amplitude are fixed; only the strength of the random walk in phase is varied. We then compare the simulations with the power spectrum of the real data to deduce the degree of phase noise present.

An example of this procedure is illustrated in Figure 9 which shows three power spectra generated by

$$f(t) = 100 + 20 \cos(\omega t + \phi_t) + 20 \cos[2(\omega t + \phi_t)]. \quad (9)$$

Here ϕ_t is a step function which changes its value every cycle:

$$\phi_t = \phi_{t-P_0} + \frac{2\pi P_1}{P_0} x,$$

where P_0 is the basic pulsation period, chosen for Figure 9 to be 25 s; P_1 can be thought of as the standard deviation

of the pulsation period and is related to S by equation (1) in Paper I; and x is a random variable distributed according to a Gaussian function (of zero mean and unit standard deviation) that is different for each cycle. A term for the second harmonic has been included to test for sensitivity to pulse shape information in the presence of phase noise. We have chosen values for P_1 equal to 1.5, 3, and 5 in Figures 9a, 9b, and 9c, respectively. The artificial data set consisted of 256 pulses.

A comparison of the power spectrum of the real SS Cyg data with such simulated data (using an appropriate value for P_0) gives an estimate of the strength of the phase noise. The procedure has been tested on the data from the 1978 SS Cyg and the U Gem observations and gives results that agree with the previous methods. The parameters for the 1979 SS Cyg observation derived in this way are: $I \sim 0.02$ counts $\text{cm}^{-2} \text{s}^{-1}$, $A \sim 0.18$, $P \sim 10.7$ s, and $S \sim 0.1$. This is in dramatic contrast with the 1978 SS Cyg observation when the period was somewhat shorter (8.8 s), the intensity and pulsa-

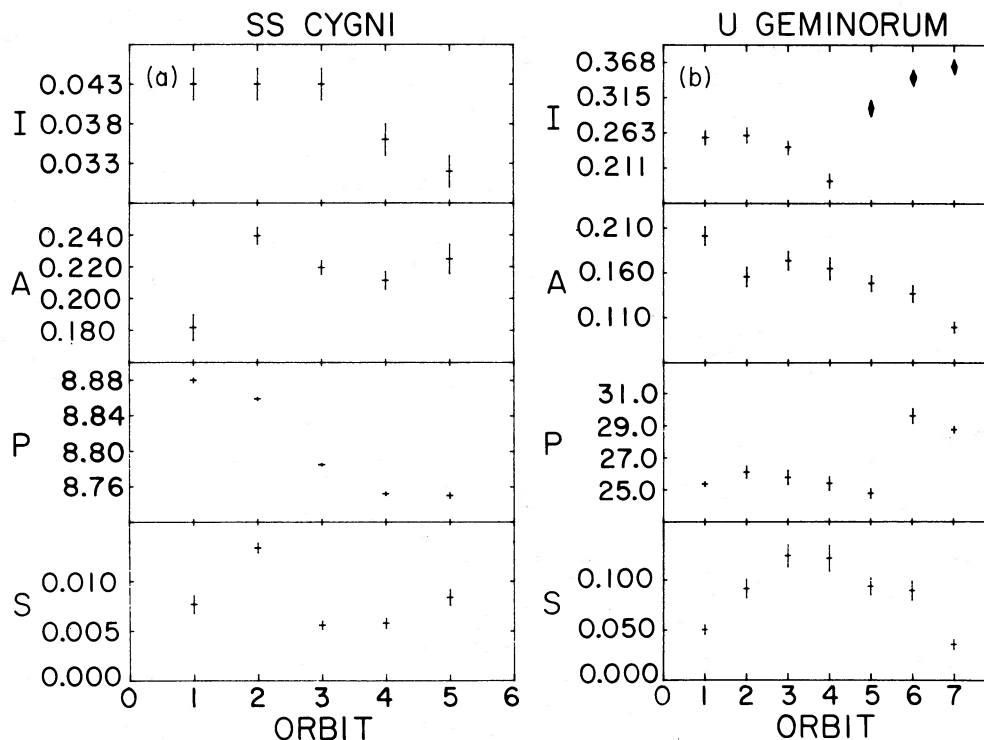


FIG. 8.—The soft X-ray intensity, pulsed fraction (including white noise), period of the pulsation, and strength of the random walk in phase plotted versus time for (a) SS Cyg (1978 June observation) and (b) U Gem. In Fig. 8b the last three points in the intensity plot were taken at a different detector gain than the first four points (see Fig. 2).

tion amplitude twice as high, and the noise strength 10 times lower.

Finally, a word of caution. The disadvantages of using the power spectrum analysis are many: the power spectrum is contaminated by amplitude noise; the parameters must be derived by subjectively comparing data; it is difficult to obtain formal uncertainties in the derived parameters; and, as illustrated in the sequence in Figure 9, harmonics are preferentially washed out as the degree of phase noise increases. The pulse superposition method described in § IIIa provides a more sensitive measure of harmonic content. In view of these difficulties, the technique of comparing power spectra with simulations should be used only as a last resort.

IV. DISCUSSION

a) Comparison of Optical and X-Ray Oscillations

To date, SS Cyg and U Gem are the only dwarf novae in which intense soft X-ray emission has been observed during optical outburst (Córdova *et al.* 1980b; Córdova and Mason 1983b), and in both of these systems the soft X-rays have been found to undergo quasi-periodic pulsations.⁷ Information concerning soft X-ray pulsations in SS Cyg and U Gem is summarized in Table 1. The visual brightness of the stars during the X-ray observations is also listed in Table 1; this should be compared with the mean quiescent state magnitudes

⁷ U Gem has been subsequently observed twice in outburst using the *Einstein X-Ray Observatory*. In one of the observations, a marginally significant pulsation (3σ) was detected at a period of 21 s and an amplitude of $\sim 12\%$, but in the other observation no evidence for pulsations was found between 20 s and 30 s with a 3σ upper limit of 5% (Córdova and Mason 1984).

of ~ 11.8 and ~ 14.5 for SS Cyg and U Gem, respectively. The X-ray oscillation periods of SS Cygni are in the same range as the optical periods detected in this star (see below), but no time-resolved simultaneous observations of SS Cyg have yet been conducted in the two bands. No short period optical pulsations have been reported for U Gem, although longer period quasi-periodic variability has been observed (RN). The average amplitudes of the X-ray pulsations are very high (15%–30%) compared to the average amplitudes of the optical oscillations ($\leq 2\%$). In Table 1 the coherence of the pulsations is given in two different (model-dependent) notations: the “S” value (see § IIIa), and the e -folding time of the autocorrelation function measured in pulsation cycles (where cycles = $[\gamma P_0]^{-1}$; cf. Appendix). The Appendix describes how these and other coherence parameters used commonly in the literature are related. The important point to note is that a wide range of coherence values has been observed for the same star at different times.

Table 2 lists the optical observations of SS Cyg and U Gem for which we have been able to determine, from the published data, the coherence times of the oscillations. Because of numerical errors, the coherence values given by HSS (see their Fig. 6) are too large by a factor of π and have been corrected in Table 2.

From a comparison of Table 1 and Table 2 it is clear that the decay times of the observed X-ray oscillations of SS Cygni are shorter than those of the observed optical oscillations at the same period. In fact, the coherence of the X-ray oscillations in both SS Cyg and U Gem is more typical of the longer period “quasi-coherent” oscillations seen in these and

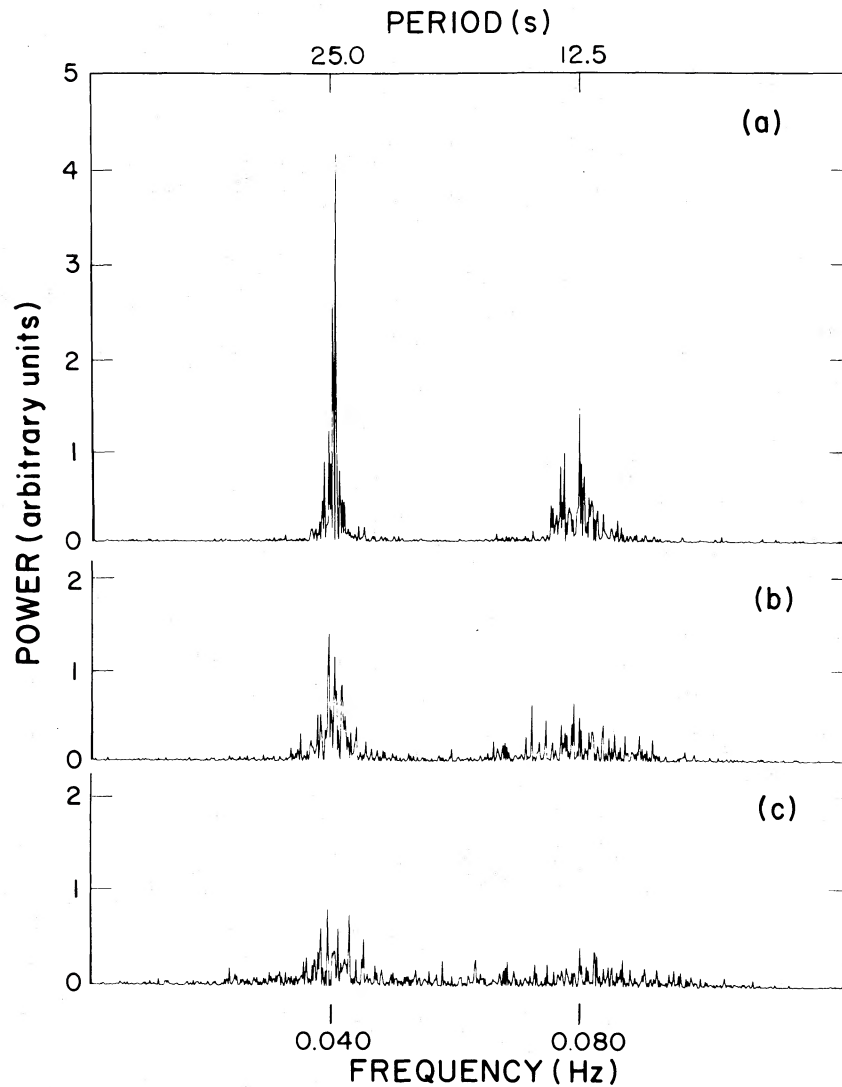


FIG. 9.—Power spectra generated from artificial data to show the effect on a sinusoid and an equal-amplitude first harmonic of increasing the phase noise. In Fig. 9a the strength of the random walk is approximately the same as in the 1978 June observation of SS Cyg, in Fig. 9b it is about 4 times greater, and in Fig. 9c it is more than 11 times greater. Fig. 9c most nearly resembles the power spectra of U Gem, and SS Cyg during the 1979 January observation (cf. Figs. 4 and 6). The series of figures illustrates that the second harmonic is washed out even more than the fundamental when the phase noise is increased, and that period shifts and multiple pseudo-periodicities (spikes in Fig. 9c) can result from a random walk of the phase.

other dwarf novae than of the “coherent” oscillations (cf. definitions in RN). If the X-ray and optical pulsations have a common origin and are usually relatively incoherent, the apparent difference in their average coherence values could be a selection effect. X-ray pulsations would typically be detected, but with low coherence. The amplitude of the optical pulses is much lower, however, and they would be detectable only when the coherence is high. Alternatively, the X-ray pulsations may originate in a completely different way from the optical pulsations and could be intrinsically less coherent.

The first four entries in Table 2 are measurements made consecutively over the course of a few days during the decline of SS Cyg from an outburst. They show that the coherence time scale of the short period optical oscillation decreased from ≥ 400 cycles to ~ 50 cycles. It may be that the observed “disappearance” of dwarf nova pulsations at the end of out-

bursts (e.g., Patterson 1981) is related to a degradation in the pulse coherence, so that the pulsations become indistinguishable from flickering.

The coherence of the oscillations in SS Cyg is not a single valued function of the period (cf. Fig. 3 in Córdova and Mason 1982). A coherence/luminosity relationship similar to the period/luminosity relationship with its hysteresis-like behavior may be operating (see examples in Patterson 1981): i.e., the coherence may reach a maximum at some point during the course of an outburst. Additional observations through an outburst, preferably of an X-ray pulsation because of its much higher amplitude, are required to test this.

b) *The Origin and Nature of the Pulsations*

The dwarf nova pulsations have been variously attributed to density or temperature enhancements rotating with the

TABLE 1
SOFT X-RAY OBSERVATIONS OF PULSATIONS OF DWARF NOVAE

| OBJECT | DATE | V MAG. | P_0 (s) | AMPLITUDE (%) | COHERENCE | |
|--------------|---------------|--------|--------------|------------------|-----------|----------|
| | | | | | (S) | (cycles) |
| SS Cyg | 1978 Jun 14.8 | 8.3 | 8.8 | 30 | 0.008 | 28 |
| U Gem | 1978 Oct 16.4 | 10.0 | ~27 | 15 | 0.08 | 1 |
| SS Cyg | 1979 Jan 4.0 | 9.1 | ~11 | 18 | 0.10 | 2 |

Keplerian period of the inner disk (Bath 1973); disk oscillations whose periods correspond to the Keplerian periods of the oscillating disk annuli (RN; Van Horn, Wesemael, and Wignat 1980; Cox 1981); normal modes in the atmosphere of the white dwarf, perhaps excited by interaction with the disk (Papaloizou and Pringle 1978, 1980); and accretion instabilities in the boundary between the disk and the white dwarf, perhaps magnetically controlled (e.g., Paper I).

Each of these models has a characteristic time scale and coherence that can be favorably compared with some of the observed pulsations, but, as discussed in Paper I, no model satisfactorily explains the details of all of the pulsations. The oscillations that are found in optical light may consist of either direct or reprocessed light. If the latter is true, the short period of the oscillations does not necessarily constrain the location of the reprocessing region in the binary system. The high amplitude and short period of the soft X-ray pulsations, however, require that these must be directly emitted from the immediate vicinity of the white dwarf.

i) *Mathematic Models and the X-Ray Constraints*

The pulsations in cataclysmic variables have been described mathematically in a number of ways, each of which can produce Fourier spectra and light curves similar to those observed. We examine below three such mathematical descriptions and discuss what constraints are imposed on them by the X-ray data.

Randomly Excited Damped Harmonic Oscillator (Model 1).—

The dwarf nova oscillations can be patterned with an autoregressive (AR) process, whose mechanical analogue is a damped harmonic oscillator excited by small, random displacements (RN). The power spectrum of a signal produced by such a process is a Lorentzian whose half-width at half-maximum is a measure of the decay time of the oscillation. Such a distribution has been fitted to the quasi-coherent oscillations of a few dwarf novae by RN and to the more coherent 7 s optical oscillation of SS Cyg by Hildebrand, Spillar, and Stiening (1981, hereafter HSS). For an AR process the standard deviation of the power is equal to the power itself (RN). It is thus not difficult to represent almost any of

TABLE 2
OPTICAL OBSERVATIONS OF PULSATIONS OF SS CYGNI AND U GEMINORUM

| Object | V Mag. | P_0 (s) | Amplitude (%) | Coherence (cycles) | References |
|--------------|--------|--------------|------------------|-----------------------|------------------|
| SS Cyg | 8.3 | 7.5 | ≤0.07 | >400 | HSS ^a |
| | 8.2 | 7.3 | ≤0.07 | 270 to >410 | |
| | 8.5 | 7.5 | ≤0.07 | 133 | |
| | 9.0 | 9.0 | ≤0.07 | 52 | |
| | 8.5 | 8.2 | 0.05 | 329 | HG ^b |
| | 8.6 | 8.5 | 0.06 | 459 | |
| | 8.5 | 9.7 | 0.02 | >410 | PRK ^c |
| | 8.5 | 31.5 | 0.3 | 5 | RN ^c |
| | 8.9 | 9.9 | 0.11 | ? | GIO ^d |
| | 8.7 | 9.7 | 0.11 | ? | |
| | 8.5 | 9.2 | 0.11 | ? | |
| U Gem | 8.4 | 9.0 | 0.18 | ? | RN ^e |
| | ... | 73 | 0.8 | 4 | |
| | ... | 90 | ? | ? | |
| | ... | 76 | ? | ? | |
| ... | 146 | 3 | ? | RN ^f | |

NOTE.—Each group of observations refers to a single outburst; the entries are listed sequentially.

^a Measurements were made over 7 days during outburst peak and decline.

^b Measurements were made 8 and 10 days after start of an outburst in which peak V magnitude was 8.5.

^c Both pulsations were detected during the same time interval.

^d Measurements were made over 4 consecutive days during rising portion of the outburst.

^e Measurements were made 13–18 days after peak V magnitude of 9.2 had been reached.

^f Measurements were made 14 days after peak V magnitude of 9.1 had been reached.

the dwarf nova power spectra as an AR process—even if the oscillation appears to be quite coherent, making it hard therefore to exclude this model. If the AR model is to be applied to the 1978 SS Cyg data, however, its parameters are constrained by the absence of large phase jumps in the times of pulse maxima seen in the data (see Paper I, Fig. 6). In the AR model, oscillations can be excited at any random phase. Thus there must be enough independent pulse trains present at any one time so that the sudden appearance of a new pulse train does not cause a phase jump in the resulting data that is larger than those seen. (The pulse phase in the first SS Cyg observation changes relatively smoothly and is confined to a relatively small range in phase angle.) At the same time, the amplitude of the SS Cyg pulsations during this time is consistently very high. There cannot therefore be too many independent pulse trains present simultaneously, or they would tend to cancel each other out and yield a relatively low-amplitude modulation.

The Phase Noise Model (Model 2).—A mathematical model which can produce pulsations whose phase evolves in the way observed for SS Cygni's X-ray pulsations (Paper I) and RU Peg's 50 s optical oscillation (Patterson, Robinson, and Nather 1977) is that of a stable oscillator whose phase is disturbed in a random manner (§ IIIb). As is illustrated in Figure 9, a variation in the strength of the "phase noise" can dramatically affect the coherence of a pulsation: Figure 9a shows a strong pulsation with an appearance similar to that of the first (1978) SS Cyg X-ray observation; Figure 9c, on the other hand, shows only a broad enhancement in the power spectrum at periods clustering around the input period, a profile similar to that for U Gem or for the second (1979) SS Cyg observation. In Figure 9c the harmonic that showed up strongly in Figure 9a has disappeared even though its amplitude is equal to that of the fundamental. The fact that harmonics are more strongly affected by the noise in the phase than the fundamental could explain the absence of harmonics in the observed dwarf nova pulsations (Robinson 1976; Paper I). The phase noise will also have the effect of producing apparently random period shifts in limited segments of data and hence could also explain the multiple periodicities observed for almost all the dwarf nova optical pulsations in short time series (e.g., the multiple spikes in Fig. 9c).

Common to both Models 1 and 2 is that random changes in the *phase* of the oscillation produce apparent period shifts. HSS have suggested an alternate model whereby the apparent lack of coherence is caused by amplitude modulation. However, the function $F(t)$ obtained by superposing the pulse train on top of itself (§ IIIa) is insensitive to amplitude modulation, so that a modulated coherent oscillator would not produce the decay in the sinusoidal modulation that we observe. Hence this model appears to be excluded by the data. To further test this idea, J. Middleditch computed the amplitude modulation spectrum of the SS Cyg soft X-ray data of 1978 June using the method of Middleditch *et al.* (1981). He found the variation in the amplitude of the pulse is less than 50% of its average value.

Superposition of Modes (Model 3).—A much different model is the superposition of a number of modes of a stable oscillation. In a model investigated by Papaloizou and Pringle (1978, 1980), oscillatory modes are excited in the surface layer of a rapidly rotating white dwarf. The oscillation

periods, P_m , are Rossby type modes in which $P_m = P_r/m$, where P_r is the rotational period of the white dwarf surface layer, and the m 's are the azimuthal mode numbers. It is possible that the interference of the modes, or the time-dependent excitation of closely spaced modes, could produce apparent changes in phase and hence time varying Fourier transforms. In Paper I we showed how the phase of the 9 s X-ray oscillation of SS Cyg varied with time (cf. Fig. 6b in Paper I). One interpretation of these phase jumps is that they represent discontinuous changes in discrete periods, which are separated by an integer multiple of a constant period separation, ΔP . This interpretation might make sense in the context of the Rossby mode model and would then constrain P_r . The value of ΔP , 0.09, which we measure from the data in Paper I gives a value for P_r of 13 ± 2 minutes for consecutively numbered m modes centered about $m = 80$. This is actually a lower limit on P_r , since any combination of modes may be excited (e.g., only odd m , etc.). The SS Cyg data interpreted in this way require that only one discrete period is excited at a time, but it is not easy to see why a single mode rather than a spectrum of modes should be excited, or how the mode switching occurs in less than one pulsation cycle, as is required by the observations (Paper I). Another difficulty with this interpretation is the high mode numbers implied, coupled with the high observed amplitude of the X-ray oscillations. The mechanism whereby oscillations on the surface of the white dwarf might be translated into variations in the X-ray flux is unclear but presumably would take the form of a disturbance communicated to the boundary layer. When the mode number is high we would view many spatial cycles of disturbances at any one time so that the amplitude of the spatially averaged variation would be low. Only if accretion were confined to one point on the stellar surface, or the mode number were low, would we expect to see large-amplitude X-ray oscillations.

ii) Accretion Instabilities

In Paper I we suggested various ways in which the pulsation could be produced by an instability in the *rate* at which matter is accreted in the X-ray producing region. While the nature of such an instability remains speculative, it is interesting to note that accretion instabilities seem to be observed in at least two other kinds of system.

One is MXB 1730–335, from which rapid bursts of X-radiation are seen. In this system a magnetic neutron star is thought to be accreting from a nearby, low-mass companion star. One type of model attributes the bursts to the sudden inflow of material that has reached a critical density above which it cannot be supported by magnetic pressure beyond the Alfvén surface (cf. the references in Lewin and Joss 1981). In certain luminosity states, MXB 1730–335 produces quasi-periodic, low-luminosity bursts that have coherence properties similar to the oscillations in SS Cyg (e.g., Mason, Bell-Burnell, and White 1976).

A second possible example of an accretion instability is the quasi-periodic ~ 2 s variability observed in two cataclysmic variables of the AM Her class, E1405–451 and AN UMa, by Mason *et al.* (1983) and Middleditch (1982). These authors have suggested that this rapid quasi-periodic behavior might be caused by an instability in the height of the standoff shock produced when the magnetically confined accretion flow

encounters the surface of the white dwarf, an instability previously predicted by Langer, Chanmugam, and Shaviv (1981). In this model, too, the variability of the period may be related to changes in the accretion rate.

While neither of the above models may be applicable to the dwarf novae they illustrate that models of this class can reproduce similar temporal phenomena, and therefore should be explored further.

V. SUMMARY AND FUTURE OBSERVATIONS

Using the *HEAO 1* low-energy experiment, we have twice detected pulsations in the very soft X-ray flux of SS Cygni and once in U Gem. In all cases the pulsations were not strictly coherent; we have modeled the pulse instability as a random walk in the phase of the pulse. Using this model we deduced coherence time scales for the pulsations. During the first X-ray pointing at SS Cygni the observed 9 s oscillation had a coherence time of ~ 30 pulse cycles, shorter than any of the observed optical pulsations of similar period. During the U Gem and second SS Cyg pointings, the decay times of the ~ 27 s and ~ 11 s X-ray oscillations were only one to two pulse cycles, which is of the same order as the decay times of longer period "quasi-coherent" optical pulsations detected in these stars. The X-ray measurements constrain, but do not preclude, current models. It is possible that the X-ray pulsations result from changes in the rate of the accretion flow.

To further limit the selection of an appropriate description for the pulsations in dwarf novae, several observations are

badly needed: (1) the lack of observations in the EUV means that we do not know how much energy is in the pulsation; (2) the lack of simultaneous optical and X-ray timing data means that we do not know the relationship of the pulsations in the two bands and hence whether the difference in the optical and X-ray pulse coherence values is fortuitous or suggests an important constraint on the nature of the pulsation; (3) the lack of extended X-ray timing observations over the course of an outburst means that we do not know at what point during the outburst the X-ray oscillation is generated, how it finally decays, or how it is related to the bolometric luminosity of the system; and (4) the observation of high-energy pulsations in only two dwarf novae limits our understanding of the pulsation mechanism—and indeed the production of X-rays—and again points to the promising EUV band as a source of more information about the inner accretion disk/white dwarf region.

We are very grateful to Mr. Jim Morgan and Dr. Janet Mattei for alerting us to the optical outbursts of these dwarf novae and to the AAVSO for providing the data used to construct the visual light curves. We thank the anonymous referee for detailed comments on an early version of this manuscript. Dr. John Middleditch is acknowledged for calculating the power spectrum of the amplitude modulation in SS Cyg. This research was supported by NASA contracts NAS 5-25049 and NAGW-44, the US Department of Energy, and the UK S.E.R.C.

APPENDIX

The coherence values for quasi-periodic dwarf nova oscillations reported in the literature have been derived in the context of various mathematical models and consequently are expressed in terms of different parameters. However, these parameters can be simply related, as we explain here. In Tables 1 and 2 we have made use of these equivalences to compare the decay times of all the SS Cygni and U Geminorum pulsations reported at both optical and X-ray wavelengths.

1. As illustrated previously, one description of the coherence of a pulsation is the parameter S , where $S = R\langle\Delta\phi^2\rangle$, or the rate at which the phase is stepped times the mean square phase step. Horne and Gomer (1981) parameterize their measurements of optical pulsations in SS Cyg with σ , the expected phase walk in one cycle. From the above definition for S , it can be seen that this measurement is related to S by: $S = P_0^{-1}[(\pi/180)\sigma]^2$, where P_0 is the oscillation period.

2. RN use an autocorrelation technique to find the pulsation parameters of the quasi-coherent optical oscillations of dwarf novae. The mathematical process used by RN to produce a light curve similar to the quasi-periodic oscillation light curve [cf. § IVb(i)(Model 1)] yields an autocorrelation function.

$$r_\tau = e^{-\gamma\tau} \cos \omega\tau,$$

i.e., a cosine with an exponentially decaying amplitude. The decay time, γ^{-1} , is related to the coherence of the process giving rise to the quasi periodicity. To determine how γ is related to our S value, we have performed autocorrelations of simulated phase noise data (as per eq. [9]) and compared the ACF decay times with the corresponding S values. With this empirical method we find that $\gamma = S/2$.

3. HSS and also RN fitted a Lorentzian distribution to the power spectrum of the oscillation produced in their strongly damped noise-excited oscillator model. From HSS,

$$P(\omega) = \frac{\text{constant} \times \omega^2}{[(\omega - \omega_0)^2 + \lambda^2]}.$$

The parameter λ is related to the half-width at half-maximum of the distribution and is thus a measure of the coherence of an oscillation with a central frequency ω_0 . A comparison of the equation for the Lorentzian given above with eqs. (6) and (14) of RN shows that λ is related to γ by the expression $\lambda = \gamma/(2\pi)$, and therefore, from the previous discussion, $\gamma = S/(4\pi)$.

REFERENCES

- Arnolds, S., Berg, R. A., and Duthie, J. G. 1976, *Ap. J.*, **206**, 790.
 Bath, G. T. 1973, *Nature Phys. Sci.*, **246**, 84.
 Brown, R. L., and Gould, R. J. 1970, *Phys. Rev. D.*, **1**, 2252.
 Cordes, J. M. 1980, *Ap. J.*, **237**, 216.
 Córdova, F. A. 1979, Ph.D. thesis, California Institute of Technology.
 Córdova, F. A., Chester, T. J., Tuohy, I. R., and Garmire, G. P., 1980a, *Ap. J.*, **235**, 163 (Paper I).
 Córdova, F. A., and Mason, K. O. 1982, in *Proc. Pulsations in Classical and Cataclysmic Variable Stars*, ed. J. P. Cox (Boulder, Co.: JILA), 23.
 ———. 1983, in *Accretion Driven Stellar X-ray Sources*, ed. W. H. G. Lewin and E. P. J. van den Heuvel (Cambridge: Cambridge University Press), p. 147.
 ———. 1984, *M.N.R.A.S.*, in press.
 Córdova, F. A., Nugent, J. J., Klein, S. R., and Garmire, G. P. 1980b, *M.N.R.A.S.*, **190**, 87.
 Cox, J. P. 1981, *Ap. J.*, **247**, 1070.
 Giovanelli, F. 1981, in *X-ray Astronomy*, ed. R. D. Andresen (Dordrecht: Reidel), p. 213 (GIO).
 Hearn, D. R., Richardson, J. A., and Li, F. K. 1976, *Bull. AAS*, **8**, 447.
 Hildebrand, R. H., Spillar, E. J., and Stiening, R. F. 1981, *Ap. J.*, **243**, 223 (HSS).
 Horne, K., and Gomer, R. 1980, *Ap. J.*, **237**, 845 (HG).
 Langer, S. H., Chanmugam, G., and Shaviv, G. 1981, *Ap. J. (Letters)*, **245**, L23.
 Lewin, W. H. G., and Joss, P. C. 1981, *Space Sci. Rev.*, **28**, 3.
 Margon, B., Szkody, P., Bowyer, S., Lampton, M., and Paresce, F. 1978, *Ap. J.*, **224**, 167.
 Mason, K. O., Bell-Burnell, S. J., and White, N. E. 1976, *Nature*, **262**, 474.
 Mason, K. O., Lampton, M., Charles, P., and Bowyer, S. 1978, *Ap. J. (Letters)*, **226**, L129.
 Mason, K. O., Middleditch, J., Córdova, F. A., Jensen, K. A., Reichert, G. A., Murdin, P. G., Clark, D., and Bowyer, S. 1983, *Ap. J.*, **264**, 575.
 Middleditch, J. 1982, *Ap. J. (Letters)*, **257**, L71.
 Middleditch, J., Mason, K. O., Nelson, J. E., and White, N. E. 1981, *Ap. J.*, **244**, 1001.
 Papaloizou, J., and Pringle, J. E. 1978, *M.N.R.A.S.*, **182**, 423.
 ———. 1980, *M.N.R.A.S.*, **190**, 43.
 Patterson, J. 1981, *Ap. J. Suppl.*, **45**, 517.
 Patterson, J., Robinson, E. L., and Kiplinger, A. L. 1978, *Ap. J. (Letters)*, **226**, L137 (PRK).
 Patterson, J., Robinson, E. L., and Nather, R. E. 1977, *Ap. J.*, **214**, 144.
 Rappaport, S., Cash, W., Doxsey, R., McClintock, J., and Moore, G. 1974, *Ap. J. (Letters)*, **187**, L5.
 Ricketts, M. J., King, A. R., and Raine, D. J. 1979, *M.N.R.A.S.*, **186**, 233.
 Robinson, E. L. 1976, *Ann. Rev. Astr. Ap.*, **14**, 119.
 Robinson, E. L., and Nather, R. E. 1979, *Ap. J. Suppl.*, **39**, 461 (RN).
 Rothschild, R. E., et al. 1979, *Space Sci. Instr.*, **4**, 269.
 Swank, J. H. 1979, in *IAU Colloquium 53, White Dwarfs and Variable Degenerate Stars*, ed. H. M. Van Horn and V. Weidemann (Rochester, N.Y.: University of Rochester Press), p. 135.
 Tuohy, I. R., Lamb, F. K., Garmire, G. P., and Mason, K. O. 1978, *Ap. J. (Letters)*, **226**, L17.
 Van Horn, H. M., Wesemael, F., and Winget, D. E. 1980, *Ap. J. (Letters)*, **235**, L143.
 Wade, R. A. 1979, *A. J.*, **84**, 562.
 Warner, B. 1976, in *IAU Symposium 73, The Structure and Evolution of Close Binary Systems*, ed. P. Eggleton, S. Mitton, and J. Whelan (Dordrecht: Reidel), p. 85.

T. J. CHESTER: 1169 Meadowbrook Road, Altadena, CA 91001

F. A. CÓRDOVA: MS D436, Los Alamos National Laboratory, Los Alamos, NM 87545

G. P. GARMIRE: Pennsylvania State University, Department of Astronomy, 504 Davey Lab, University Park, PA 16802

S. M. KAHN: Physics Department, Columbia Astrophysics Laboratory, Columbia University, 538 West 120 Street, New York, NY 10027

K. O. MASON: Mullard Space Science Laboratory, Holmbury St. Mary, Dorking, Surrey, RH5 6NT, UK